Response relationship between color and chemical composition and microstructure of heat- treated wood

Meihong Liu
Forestry College, Northwest A & F University
Liangliang Zhang
Forestry College, Northwest A & F University
Jiang Chen
Forestry College, Northwest A & F University
Shuang Chen
Forestry College, Northwest A & F University
Yafang Lei
Forestry College, Northwest A & F University
Zhangjing Chen
Virginia Tech University
Li Yan (liliyan@nwsuaf.edu.cn)
Forestry College, Northwest A & F University

Research Article

Keywords: Wood heat treatment, Color, Chemical component, Cell wall microstructure, Response relationship

Posted Date: June 30th, 2023

DOI: https://doi.org/10.21203/rs.3.rs-3118054/v1

Abstract

The magnitude of the color change of heat-treated wood is closely related to the chemical composition of the wood, and the change in chemical composition is the essential reason for changes in the mechanical properties of heat-treated wood. Exploring the influence and linear correlation of the magnitude of the lightness indicator (L*) of poplar (Populus tomentosa Carr.) and spruce (Picea asperata Mast.) in heat treatment on the chemical composition and cell wall structure of heat-treated wood, and constructing a response relationship between L* values and them. The relative content of cellulose in heat-treated poplar increased gradually and was significantly negatively correlated with the L* value, however, the heat-treated spruce first increased and then decreased, and the correlation with the L* value was insignificant. The L* value of the heat-treated wood was significant positively correlated with the content of hemicellulose and lignin. The CrI and crystalline size of poplar and spruce after thermal modification first increased and then decreased with the decrease of L* value, and the L* values had a superior response relationship with their crystallite size. The shrinkage deformation and radial cracking of the cells of poplar and spruce after thermal modification became increasingly obvious as the L* value gradually decreased, the L* values had an extremely significant positive correlation with their radial thickness of the cell wall. Therefore, the constructed response relationship provides a theoretical basis for accurate and nondestructive testing of the mechanical properties of heat-treated wood using color parameters as a rapid detection indicator.

1. Introduction

The heat treatment method has the advantages of environmental friendliness, nontoxicity and simple processing, and is currently the most widely used, most successfully industrialized and economical wood modification method (Esteves et al. 2007; Sandberg et al. 2013). Thermal treatment leads to the degradation or reorganization of wood chemical compositions, which improves the decay resistance and dimensional stability of wood. (Schwarze et al. 2005; Srinivas et al. 2012; Li et al. 2021; Wang et al. 2022). In addition, the thermal treatment deepens the surface color of the wood, endowing the wood with a uniform and dignified color; thus, the ordinary wood can imitate precious wood after heat treatment and has the potential to replace precious wood (Gunduz et al. 2009).

Wood is a complex natural polymer compound mainly composed of cellulose, hemicellulose, lignin and extractives. It contains chromophoric groups such as carbonyl, carboxyl, unsaturated double bonds and conjugates as well as auxochromic groups such as hydroxyl groups. It follows that the color of wood is directly associated with its chemical components unsaturated functional groups of chemical compounds, which, under visible light, generate absorption peaks and result in the color development of chemical compounds, including vinyl, diaromatic rings, quinone, carbonyl, and phenol (Aydin et al. 2005; Tjeerdsma et al. 2005; González-Peña et al. 2009; Lu et al. 2020).

Heat treatment will change the main chemical composition of wood, resulting in an increase or decrease in its chromogenic and auxiliary groups (Okon et al. 2018; Salca et al. 2014). This is mainly due to

cellulose, hemicelluloses, and lignin experience degradation to different degrees, and oxygen-containing groups such as acetyl and carboxyl gradually degrade, leading to increased carbon content; with the degradation of hemicelluloses and cellulose, the phenolic substances go through redox reactions with increasing concentration in the heat treatment process and, as a result, the wood color darkens. As the thermal treatment temperature is increased, the lignin is degraded and thus experiences condensation reactions, the color chromophore groups in the lignin conjugate lengthen and increase in quantity (Wikberg et al. 2004; Windeisen et al. 2008). Hemicellulose is an amorphous substance in the cell wall of wood, and has many branches. Its instability leads to easy decomposition at high temperatures (generally above 150 ℃) to generate acetic acid and phenolic compounds. Phenolic compounds often contain chromophoric groups, which increase the surface color of thermal treatment wood by increasing the chromophore groups (Tjeerdsma et al. 2005; Sundqvistet al. 2006; Salca et al. 2016; Sikora et al. 2018). However, the acidic environment catalyzes the decomposition or structural change of cellulose and lignin, which promotes the cycle of this process and produces an increasing number of chromophoric substances, resulting in a decrease in the lightness index (L^*) of wood. The internal bonds of lignin are broken, which increases the content of phenolic hydroxyl groups and promotes the deepening of the color of the heat-treated wood when the heat treatment temperature is higher than 180℃. At the same time, the β-O-4 bond in lignin is broken during heat treatment to generate free radicals, which are extremely unstable in nature and interact with adjacent molecules extremely easily (Westerma et al. 1995; Sundqvist et al. 2002). Chain transfer and termination reactions generate relatively stable peroxides, which decompose into colored compounds at high temperatures, resulting in discoloration of wood (Sikora et al. 2018; Gonzalez-pena et al. 2009). In addition, lignin contains benzene ring, carbonyl, vinyl and coniferaldehyde chromophore groups, and the quinone compounds generated by the oxidation of these groups also deepen the color of the wood (Nuopponen et al. 2004; Bekhta et al. 2003; Humar et al. 2020).

Color change in heat-treated wood was related to the change in the main components of its cell wall as well as to the extent of thermal treatment (temperature and duration) (Brischke et al. 2007; González-Peña et al. 2009a; Willems et al. 2015). The changes in the chemical composition and intensities of heat treatment directly affect the properties of heat-treated wood. Therefore, the color measurement of thermally modified wood can also be used to predict and regulate properties of thermally modified wood (González-Peña et al. 2009b; Esteves et al. 2009). Yan and Morrell (2019) reported that L^* is affected by the treatment duration and temperature, and L^* is linearly negatively correlated with the treatment duration. The color parameters a^* and b^* are affected by the treatment temperature and pretreatments, but the relationship with the treatment duration and pretreatment shows a complex and nonlinear curve relationship (Bekhta et al. 2003; González-Peña et al. 2009b; Bytner et al. 2022). Torniainen et al. (2021) also proposed that the heat treatment temperature and duration can be regulated according to the L^* value of the color parameters of the heat-treated wood, and the a^* and b^* of color parameters can only be used as auxiliary parameters. Brischke et al. (2007) proposed a significant linear relationship between the weight loss rates of the heat-treated wood and their L^* and b^* values. The weight loss rate of heat-treated wood can be predicted and regulated according to the L^* and b^* values (Brischke

et al. 2007). Nasir et al. (2019a) proposed accurate prediction of the equilibrium moisture content, volumetric expansion coefficient and water absorption of heat-treated wood from the color. The mechanical properties can be predicted and regulated according to the color change of heat-treated wood. Bekhta et al. (2003) reported that there is an extremely significant linear relationship between the color difference ΔE^* and the modulus of elasticity (MOE) and modulus of rupture (MOR) of different species of heat-treated wood. The MOE and MOR of heat-treated wood can be predicted according to the value of the color difference ΔE^*. González-Peña et al. (2009b) carried out binomial fitting on the color difference ΔE^* and lightness difference ΔL^* of heat-treated wood using the MOR, MOE, hardness, shear strength, impact toughness and compressive strength. A significant correlation between both ΔE^* and ΔL^* and the mechanical properties of heat-treated wood was proposed. However, after comparative analysis, it was found that the use of ΔE^* to predict the mechanical strength of heat-treated wood was more accurate. Chen et al. (2022) from our team also proposed that a time-temperature superposition methods were used to quantify color and mechanical strength, and developed a prediction model of the heat-treated material color parameters with their MOR, MOE, and shear strength. In addition, some scholars have also proposed that the color of heat-treated wood can be used to quickly classify heat-treated hardwoods (Willems et al. 2015; Schnabel et al. 2007; Nasir et al. 2019b).

Compared with other performance evaluations of heat-treated wood, color measurement has been investigated as a potential nondestructive evaluation method for the quality control of thermally modified wood (Torniainen et al. 2021). Previous studies have focused on establishing the correlation between the color and the intensities of heat treatment and the physical and mechanical properties of heat-treated wood. However, there has been little analysis of the correlation between the color parameters of heat-treated wood and its main components and the microstructure of the cell wall. The color change of heat-treated wood is mainly due to degradation of the main components of the cell wall and the extracts caused by heat treatment, which result in color changes of the heat-treated wood (Salca et al. 2016; Okon et al. 2018). However, the change in the main components and microstructure of the cell wall is the essential reason for the change in the physical and mechanical properties of the heat-treated wood (Hillis et al. 1984; Obataya et al. 2000; Yildiz et al. 2006; Akgul et al. 2007; Korkut et al. 2008). In addition, it has been suggested that there is controversy regarding the effectiveness of color measurements for predicting wood mechanical properties (Johansson et al. 2006). The objective of this study is to explore the correlation between the color and the principal components and microstructure of the cell wall of heat-treated wood and constructed the relationship between the color and microstructure and principal components of the heat-treated wood. The constructed response relationship provides a theoretical basis for constructing the response relationship between the color and the physical and mechanical properties of heat-treated wood. In addition, it provides a new approach to accurately and nondestructively test the performance of thermal treatment wood using the color parameters as a rapid detection indictor and provides a new avenue for the study of color response and the performance of treated wood in the field of functional improvement of wood.

2. Materials And Methods

2.1. Materials

Poplar (*Populus tomentosa* Carr.) log was harvested from plantation at Northwest A&F University in the Yangling District, Shaanxi Province, China, with a diameter of more than 43 cm at breast height. One hundred and thirty clear flat-sawn boards with dimensions of 20 mm × 100 mm × 390 mm (radial (R) × tangential (T) × longitudinal (L)) were sawn. Spruce (*Picea obies* Mast.) lumber was imported from Finland as flat-sawn boards with dimensions of 25 mm × 300 mm × 4000 mm (R × T × L) (130 samples). The boards were dried in an oven at 60 °C to 12% moisture content (MC). Then, the dried poplar and spruce boards were randomly divided into 13 groups with ten in each group. One group was randomly selected as the control group, and the other 12 groups were subjected to thermal modification at different heat treatment temperatures and times. The chemicals used in the experiments include sulfuric acid (Luoyang Haohour Reagent Co., Ltd.), anhydrous ethanol (purity ³ 99.7%, Chengdu CHRON Chemical Reagent Factory), potassium bromide (purity ³ 98.08%, Sunshine Biotechnology Co., Ltd.), calcium carbonate (Tianli Reagent Co., Ltd.), glucose and xylose standards (Sigma–Aldrich, USA).

2.2. Thermal treatments

Using air as the heating medium, the designed heat treatment temperature and heat treatment time were tested as two factors at multiple levels to heat the poplar and spruce in the thermal chamber. The design of the thermal treatment time and temperature process parameters is shown in **Table 1**.

Table 1 Temperature and time parameters of the thermal treatment.

Group number	Species	Temperature (°C)	Duration (h)
1	Poplar	180	4
2	(*Populus tomentosa* Carr.)		6
3			8
4			10
5		200	2
6			4
7			6
8			8
9		220	2
10			4
11			6
12			8
1	Spruce	180	2
2	(*Picea obies* Mast.)		4
3			6
4			8
5		200	2
6			4
7			6
8			8
9		220	2
10			4
11			6
12			8

2.3. Surface color parameters

The color parameters of poplar and spruce before and after the heat treatment were determined using the CIE $L^*a^*b^*$ color space system with a CHNspec CS-802 spectrophotometer, where the L^*, a^*, and b^* coordinates represent the lightness, red-green color pair, and yellow-blue color pair, respectively. The dimensions of the end-matched samples were 20 × 100 × 390 mm^3. A scanning hole with a diameter of

25 mm was selected for the colorimeter. For each sample, 9 nonoverlapping points were selected for testing. Ten samples were analyzed for each group, and the test results were averaged.

2.4. Determination of wood chemical components

The untreated wood and thermal treatment wood were ground into 40-60 mesh powder. Then, the powder was oven dried to constant weight at 60 °C and put into a dryer for use.

Glucose standards and xylan standards were prepared. Concentrated sulfuric acid was prepared as a mobile phase with a concentration of 5 mmol/L, and glucose standards and xylan standards were prepared as 2 mg/ml standard solutions. Then, equal amounts of glucose and xylan standards were mixed. The mixture of glucose and xylan standard solution was diluted with sulfuric acid mobile phase to different concentrations **(Table 2)**.

Table 2 Standard solutions of glucose and xylose at different concentrations.

Element	Concentration (mg/ml)			
	0.05	0.20	0.40	0.60
Glucose (2 mg/ml)	25 µl	100 µl	200 µl	300 µl
Xylose (2 mg/ml)	25 µl	100 µl	200 µl	300 µl
Sulfuric acid mobile phase	950 µl	800 µl	600 µl	400 µl
Total capacity	1 ml	1 ml	1 ml	1 ml

The linear regression equation of the monosaccharides is shown in **Table 3**. The linear correlation coefficient R^2 of glucose and xylan both reached 0.999.

Table 3 Linear regression equations of monosaccharides.

Types of monosaccharide	Linear regression equation	Correlation coefficient (R^2)	Linear range (mg/ml)
Glucose	y = 193,911.0909 x + 133.1091	0.9996	0.05-0.60
Xylose	y = 184,027.9273 x +466.7727	0.9998	0.05-0.60

Acid hydrolysis of poplar and spruce wood powder was performed before and after heat treatment. First, the filter paper used in the experiment was extracted with a Soxhlet extractor, and the extracted filter paper was dried in a drying oven at 60 °C to a constant quality, mainly to avoid the effect of the filter paper extract on the acid hydrolysis of wood. The 200-mesh wood powder was wrapped with the extracted filter paper and placed in a Soxhlet extractor. Then, 200 ml of absolute ethanol was added to a 250 ml round-bottomed flask, the oil bath temperature was set to 95 °C, Soxhlet extraction was performed for 48 h (guaranteed to reflux once every 10 min) until the reflux liquid was colorless and transparent, and

the extract in the wood powder was completely removed. The extracted wood powder was oven dried at 60 °C to constant weight. Subsequently, 300 mg of the extracted and dried wood powder was transferred into a silk-neck bottle. Next, 3 ml of 72% sulfuric acid was added, shaken well, and fully acid hydrolyzed in a water bath at 30±3 °C for 60 min (shaken well every 5 minutes). After the first step of complete acid hydrolysis, 84 ml of distilled water was added to the silk-neck bottle to dilute the sulfuric acid to 4%. After tightening the cap, the silk-top bottle was placed in an autoclave and hydrolyzed at a temperature of 121 °C for 60 min to complete the second step of acid hydrolysis. After the hydrolysis was completed, a G3 sand core funnel was used for suction filtration after complete cooling. The filtrate and residue were stored separately, and the content of cellulose, xylan, acid-insoluble lignin and acid-soluble lignin of the wood were determined.

2.5. The main components of the wood cell wall analysis

The content of cellulose, hemicellulose and lignin of poplar and spruce before and after heat treatment were analyzed using the high-performance liquid chromatography (HPLC) analysis based on the standard procedure from the National Renewable Energy Laboratory (NREL) (Yang et al. 2007; Ge et al. 2020).

2.6. Fourier transform infrared analysis (FTIR)

To examine the change in functional groups and the generation of new functional groups in the poplar and spruce before and after heat treatment, the infrared spectra of the samples were obtained by FTIR spectroscopy (Nicolet 6700, Thermo Scientific, USA). The sample size was 200 mesh powder, and three specimens were tested in each set of replicates, and the mean spectra of the specimens was calculated by averaging the three spectra. The data processing of the infrared absorption curve of wood powder was carried out using OMNIC software with the testing instrument.

2.7. X-ray diffractometer analysis (XRD)

The XRD instrument from D/max-2500/PC (Japan Science Corporation) was used (Cu- radiation (l = 0.154 nm) with a graphite monochromator, electric current 40 mA, voltage 40 kV) with a 2 scan range from 5 to 40 at a scan speed of 4 /min. The crystallinity index (C_rI) was determined using the peak height method developed by Segal *et al.* (1959). The Scherrer formula, Eq. 1 (Scherrer 1918; Wei et al. 2015) was used to measure the crystallite size, L_{200}.

$$C_rI = \frac{I_{002} - I_{am}}{I_{002}} \times 100\% \quad (1)$$

$$L_{200} = \frac{k\lambda}{\beta_{1/2}\cos\theta} \quad (2)$$

In Eqs. 1 and 2, is (002), the maximum intensity of the crystalline diffraction angle; is the scattering intensity of the noncrystalline background diffraction at approaching 18 ; is the crystallite size (nm); is the incident wavelength, taken as 0.154 nm; *k* denotes the diffraction constant (0.90); indicates the peak

width of the (200) profile at half-maximum (FWHM) in radians; and θ indicates half of the (200) Bragg diffraction peak position (2θ max position) in radians. The FWHM and peak position for the (200) reflection was measured from the diffractograms of the samples after a Gaussian profile function was fitted between 2θ *values* of 18 and 29 Two hundred-mesh poplar tomentosa and spruce wood powders before and after heat treatment were prepared for X-ray diffraction experiments, with 3 replicates for each group of samples.

2.8. Scanning electron microscopy (SEM)

The transverse surface morphologies of the poplar and spruce before and after heat treatment were represented by a Hitachi SU 8010 field emission scanning electron microscope (FE-SEM). Thin-slice samples of untreated and thermally modified wood with a thickness of 2 mm and dimensions of 10 mm × 10 mm × 10 mm were observed and subsequently dried in a drying oven at 60 °C for 24 h. The radial thickness of the wood cell walls was measured using scanning electron microscopy data manager software by obtaining SEM images. The cell wall radial thickness of at least 200 cells was tested for each sample, and the test results were averaged.

2.9. Statistical analysis

Using IBM SPSS Statistics 25.0 analysis software, the color parameters L^*, a^*, b^* of the poplar and spruce under different heat treatment conditions were subjected to univariate post hoc multiple comparison analysis (LSD). The Pearson correlation between the lightness L^* of thermally modified wood and the content of the main components of the cell wall and radial thickness of the cell wall were analyzed.

3. Results And Discussion

3.1. Surface appearance and color parameters

The surface colors of the poplar and spruce samples treated under different treatment conditions are shown in **Figure 1**. The thermally modified wood surface color gradually deepening with increasing heat treatment duration and temperature. The higher the thermal treatment temperature and the longer the treatment duration, the darker the surface color of heat-treated poplar and spruce was. The L^*, a^* and b^* of the color parameters of the poplar and spruce samples treated under different treatment conditions are shown in **Figure 2**. When the heat treatment temperature was fixed, the L^* of the thermal treatment wood reduced gradually with increasing treatment time, without obvious changes in a^* and b^*. When the heat treatment time was fixed, the L^* of the heat-treated wood decreased drastically, the a^* first increased and then decreased, and the b^* decreased gradually with increasing heat treatment temperature. However, compared with the change degree of the L^* value of heat-treated wood, the value of a^* and b^* didn't changes significantly with temperature and time, which is consistent with the results of previous studies. (Esteves et al. 2008; Huang et al. 2012). However, post hoc multiple comparison analysis (LSD) of the L^*, a^* and b^* of the poplar and spruce treated at different temperatures and times showed that the difference

in the L^* of heat-treated poplar and spruce between groups was extremely significant, and the changes in a^* and b^* between groups were not as significant as that in the L^* value **(Figure 2)**. Therefore, the change in the L^* value dominated the change in the color of the heat-treated material (Salca et al. 2016; Ahajji et al. 2009). In addition, it was found in our previous study that the L^* value also had an extremely significant correlation with the mechanical properties of thermal treatment wood (Chen et al. 2022). Significance analysis of the differences in the surface appearance and color parameters of the poplar and spruce after treatment under different conditions was performed for each of the 12 groups. It was determined that the L^* value of the color parameter can be used as the main research indictor to analyze the relationship between the color and the main chemicals components and microstructure of the cell wall of heat-treated wood. The response relationships between L^* and the main components and microstructure of the cell wall of the heat-treated wood were revealed. To accurately and quickly clarify the response relationships between the L^* value and the main components and microstructure of the cell wall of the heat-treated wood, among the 12 groups of heat-treated poplar and spruce, 7 groups with extremely significant differences between groups were selected for further in-depth study. The 7 groups selected for poplar were the heat treatment conditions of 180 ℃-4 h, 180 ℃-8 h, 200 ℃-2 h, 200 ℃-4 h, 200 ℃-6 h, 220 ℃-2 h and 220 ℃-8 h, abbreviated as YK-1 to YK-7, respectively. The 7 groups selected for spruce were the heat treatment conditions of 180 ℃-4 h, 180 ℃-8 h, 180 ℃-10 h, 200 ℃-4 h, 200 ℃-8 h, 220 ℃-2 h and 220 ℃, abbreviated as YS-1 to YS-7, respectively.

Note: 1-180 ℃-4h; 2-180 ℃-6h; 3-180 ℃-8h; 4-180 ℃-10h; 5-200 ℃-2h; 6-200 ℃-4h; 7-200 ℃-6h; 8-200 ℃-8h; 9-220 ℃-2h; 10-220 ℃-4h; 11-220 ℃-6h; 12-220 ℃-8h; a: poplar; b: spruce

3.2. Main components of thermally treated wood

The obtained cellulose, hemicellulose and lignin content of heat-treated poplar and spruce in relationship with the L^* value is shown in **Figure 3**. The L^* value of untreated poplar was 79.02, and that of the heat-treated poplar after YK-1 to YK-7 decreased continuously, from 61.42 to 32.23. When the L^* value decreased from 79.02 to 32.23, the relative cellulose content showed an overall upward trend, increasing from 47.57% to 61.12% **(Figure 3a1)**, the relative hemicellulose content decreased from 21.01% to 14.75%, and the relative lignin content decreased from 24.17% to 18.17% **(Figure 3a2 and a3)**. The L^* value of untreated spruce was 83.92, and that of heat-treated spruce after YS-1 to YS-7 decreased continuously, from 58.59 to 30.86. When the L^* value decreased from 83.92 to 30.86, the relative cellulose content first increased and then decreased. The possible reason is that spruce wood releases a variety of acidic volatiles during heat treatment, such as acetic acid and formic acid (Sikora et al. 2018), which partially degrade cellulose. The relative hemicellulose and lignin content in heat-treated spruce showed an overall downward trend with the decrease in the L^* value. The relative hemicellulose content was degraded more violently, decreasing from 16.81% to 8.14%, and the relative lignin content decreased from 31.54% to 21.63% **(Figure 3b1)**. The relative content of cellulose in the heat-treated wood showed an upward trend, which was mainly due to the decrease in the relative hemicellulose and lignin content, which led to the increase in the relative content of cellulose to a certain extent. Therefore, the decrease in

the L^* value of heat-treated wood was mainly affected by the degradation of hemicellulose and some lignin (Dennis et al. 2006; Welzbacher et al. 2007). Then, the equation for the relationship between the L^* value and the main composition of the heat-treated poplar and spruce was fitted using a Gaussian fit based on the variation between the L^* value and the main composition. To further analyze the response relationship between the L^* value of the heat-treated wood and the main components of the cell wall, the correlation between L^* and the content of the main components of the cell wall was analyzed by SPSS Statistics 25.0 software. The analysis results are shown in **Table 4**. The L^* of heat-treated poplar had an extremely significant negative relationship with cellulose, and the correlation coefficient was -0.868. There was an extremely significant positive correlation between the L^* and hemicellulose and lignin of heat-treated poplar, with correlation coefficients of 0.868 and 0.907, respectively. The correlation coefficient between the L^* and cellulose of heat-treated spruce was 0.211; there were significant and extremely significant positive correlations between the L^* and hemicellulose and lignin, respectively, and the correlation coefficients were 0.702 and 0.937, respectively. In summary, there is an extreme response relationship between the L^* value and the main components of the cell wall of the heat-treated wood. Therefore, by regulating the L^* value of the heat-treated wood, the main components of the cell wall can be regulated.

Table 4 Correlation analysis between L^* and the chemical composition of thermally treated poplar and spruce.

Species	Index	L^*	Cellulose	Hemicellulose	Lignin
Poplar (*Populus tomentosa* Carr.)	L^*	1			
	Cellulose	-0.868^{**}	1		
	Hemicellulose	0.868^{**}	-0.874^{**}	1	
	Lignin	0.907^{**}	-0.972^{**}	0.876^{**}	1
Species	Index	L^*	Cellulose	Hemicellulose	Lignin
Spruce (*Picea asperata* Mast.)	L^*	1			
	Cellulose	0.211	1		
	Hemicellulose	0.702^{*}	0.502	1	
	Lignin	0.937^{**}	0.272	0.739^{*}	1

Note: * and ** indicate significant correlation at the P 0.05 level and extremely significant correlation at P 0.01 level, respectively, as in the table below.

3.2. Chemical structure changes in thermally treated wood

The FTIR spectra of the control wood and thermally modified wood are shown in **Figure 4**. Compared to the control wood, the chemical structure of heat-treated poplar and spruce wood were changed. The peaks of 3404 cm^{-1} and 3401 cm^{-1}, 2922 cm^{-1} and 2901 cm^{-1}, and 1735 cm^{-1} and 1732 cm^{-1} refer to the stretching vibration of hydroxyl (-OH), C-H stretching of cellulose, and C=O stretching vibrations in acetyl, carbonyl and carboxyl groups present in lignin and hemicelluloses, respectively (Colom et al. 2003; Cademartori et al. 2013). The intensity of these peaks was reduced as the L^* value of thermally modified wood decreased. The decrease in the peak intensity of -OH was mainly attributed to the dehydration of the hydroxyl groups between the cellulose molecular chains to generate ether bonds (Moharram et al. 2008; Yang et al. 2007). The peak intensity of C-H in the methyl and methylene groups in the cellulose molecular chain decreased slowly, which indicates cellulose degradation and an increase in its crystalline fraction during the thermal modification process (Spiridon et al. 2011). The decrease in the intensity of C=O is likely due to decarboxylation and decarbonylation reactions within the structures of cellulose and hemicellulose (Xu et al. 2019). The acetyl group ($CH_3C=O$) on the polysaccharide molecular chain of hemicellulose is broken, reducing the carbonyl group (C=O). However, the acetic acid formed by the cleavage of the acetyl group can catalyze the hydrolysis of polysaccharides as well as cause the esterification of lignin, resulting in a decrease in the number of hydroxyl groups (Kamdem et al. 2002; Mitchell et al. 2007). The removal of the acetyl group is also evidenced by the reduction in the intensities of the absorption bands at 1264 cm^{-1}, 1260 cm^{-1} and 1240 cm^{-1}, 1239 cm^{-1}. This originates from the combination of the C-O stretching vibration of Ph-O-C (Ph: p-hydroxyphenyl) in lignin, the coupling of aromatic ring vibrations and the C-O stretching vibration of xylan in hemicellulose (Popescu et al. 2013; Vartanian et al. 2015). For the heat-treated spruce, the peak intensity of the C=O absorption band was greatly decreased when compared to the heat-treated poplar, which is due to the greater degradation of hemicelluloses in the heat-treated spruce. This result is consistent with that of the NREL analysis. The peak intensities of the hydroxyl and carbonyl groups of the thermally modified wood continued to decrease, indicating a certain reduction in the hemicellulose and cellulose content (Tjeerdsma et al. 2005).

The major lignin bands in the lignin structure are at approximately 1508 cm^{-1} and 1509 cm^{-1}, 1422 cm^{-1} and 1426, and 1260 cm^{-1} and 1264 cm^{-1} (Faix et al. 1991). The peaks of 1508 cm^{-1} and 1509 cm^{-1} and 1422 cm^{-1} and 1426 cm^{-1} refer to the C=C stretching vibration of the benzene ring aromatic skeleton and aromatic skeletal vibration in lignin with C-H deformation and carbohydrates, respectively (Popescu et al. 2013; Özgene et al. 2017). The peaks at 1508 cm^{-1} and 1509 cm^{-1} show a weak decrease with the reduction in the L^* value of thermally modified wood. This band is associated with syringyl and guaiacyl units in wood lignin. A decrease in absorbance is due to the loss of syringyl units, the breaking of aliphatic side chains or the decrease in methoxyl groups (Esteves et al. 2013). The peaks at 1422 cm^{-1} and 1426 cm^{-1} showed a slight decrease, which is caused by lignin degradation and the cleavage of methoxyl groups during thermal modification (Kacik, et al. 2016). There was an obvious absorption peak at 1040 cm^{-1}, which is the overlap area between cellulose and lignin. These peaks were assigned to symmetric C-O-C stretching of dialkyl ethers, C-O ester stretching vibrations in methoxy groups, C=O

deformations in cellulose, aromatic C=H deformations in lignin, and β-O- 4 bonds. However, the peak intensity declined as the L^* value of thermally modified wood decreased. This indicates that thermal modification destroys the lignin molecular structure to a certain extent, and it was shown that the lower the L^* value of thermally modified wood was, the greater the destruction degree (Hakkou et al. 2006; Esteves et al. 2013; Popescu et al. 2013; Zheng et al. 2015; Özgenç et al. 2017). Based on the FTIR results, it can be concluded that there was an important response relationship between the L^* value and the main components of the cell wall of the thermally modified wood. The degradation degree of the main components of the cell wall after thermal modification can be regulated according to the L^* value.

3.3. X-ray diffraction

Thermal modification degraded the main chemical components of wood and changed the crystallinity and microcrystalline morphology of cellulose. The XRD diffractograms, relative crystallinity, and width of the crystalline regions of the untreated and treated wood samples are shown in **Figure 5a1 and b1**, respectively. The crystallographic planes of crystals from typical crystalline cellulose I structures have been identified as (101), (002), and (040), and their corresponding diffraction angles (2θ) from X-ray diffraction (XRD) are 15.75°-16.20°, 22.08°-22.37°, and 34.45°-34.52°, respectively (French et al. 2014; Poletto et al. 2012). For the untreated wood, the positions of the diffraction peaks of the cellulose crystal plane (002) of the poplar and spruce under different heat treatment conditions did not change by approximately 22.0°. This indicates that the crystalline structure of the poplar and spruce was not destroyed during the heat treatment process. However, after thermal modification of the wood, there was a significant increase in the intensity of the (002) reflection, indicating that the thermally modified wood became more crystalline than the untreated wood.

The *CrI* and crystallite size of the samples are shown in **Figure 5a2 and b2**. Thermally modified wood showed a higher *CrI* than untreated wood. After heat treatment, the *CrI* of poplar first increased and then reduced with reducing L^* value. When the L^* decreased from 61.42 (YK-1) to 37.55 (YK-6), the *CrI* increased from 46.96% (YK-1) to 60.18% (YK-6). However, when the L^* decreased from 37.55 (YK-6) to 32.23 (YK-7), the *CrI* declined from 60.18% (YK-6) to 52.63% (YK-7). The *CrI* of the untreated spruce was 40.90%. After thermally modification, the *CrI* first increased and then reduced with decreasing L^* value. When the L^* decreased from 58.59 (YS-1) to 34.15 (YS-5), the *CrI* increased from 43.00% (YS-1) to 51.45% (YS-5). However, when the L^* decreased from 34.15 (YS-5) to 30.86 (YS-7), the *CrI* declined from 51.45% (YS-5) to 44.31% (YS-7). The increase in the *CrI* of wood caused by thermally modification is mainly attributed to the crystallization of quasicrystals in the amorphous region caused by the rearrangement or reorientation of cellulose molecules (Toba et al. 2013; Endo et al. 2016). The second cause is the poor thermal stability of the amorphous region. During the thermal modification process, the molecules in the amorphous region of cellulose and hemicellulose are degraded, and the hydroxyl groups dehydrate and form ether bonds, which makes the arrangement of the microfibrils in the amorphous region more orderly, moving closer to the crystalline region and orientation, and increases the crystallinity of cellulose. (Akgul et al. 2007; Zheng et al. 2013; Lin et al. 2018). Notably, the *CrI* of poplar and spruce of thermal

modification declined as the L^* value further decreased. Similar phenomena were found in other studies (Zheng et al. 2013), mainly due to the large hydrolysis of hemicellulose to produce acetic acid. Acetic acid degrades the microfibrils in the amorphous region (and even the shaped region of cellulose) and hydrolyzes the glucose unit into a short-chain structure, thereby reducing the relative crystallinity of the heat-treated cellulose (Bhuiyan et al. 2000). The increase in *CrI* is mainly caused by an increase in crystalline regions or a decrease in amorphous regions. From the change in the crystallite size, it can be determined whether the increase in *CrI* is due to the former or the latter. By exploring the relationship between the crystallite size and L^* value of the thermally modified wood, a theoretical basis was provided for constructing the response relationship between the L^* value and the *CrI* of thermally modified wood. The crystallite size increased first and then decreased with the decrease in the L^* value of the heat-treated wood, which is consistent with the change trend of *CrI*. The crystallinity region width of the untreated poplar was 2.23 nm. When the L^* of the heat-treated poplar decreased from 61.42 (YK-1) to 37.55 (YK-6), the crystallinity region width increased from 2.26 nm (YK-1) to 2.45 nm (YK-6). However, when the L^* decreased from 37.55 (YK-6) to 32.23 (YK-7), its crystallinity region width declined from 2.45 nm (YK-6) to 2.39 nm (YK-7). The crystallinity region width of the untreated spruce was 2.25 nm. When the L^* of heat-treated spruce decreased from 58.59 (YS-1) to 50.64 (YS-3), the crystallinity region width increased from 2.27 nm (YS-1) to 2.36 nm (YS-3). However, when the L^* decreased from 50.64 (YS-3) to 30.86 (YS-7), the crystallinity region width declined from 2.36 nm (YS-3) to 2.27 nm (YS-7). The amorphous regions in the heat-treated poplar cellulose were arranged more closely and orderly, which enlarges the size of the crystalline regions of the cellulose. Therefore, the increase in the *CrI* was caused by the increase in the crystalline regions. The crystallite size of the heat-treated spruce began to decrease when the L^* decreased to 42.42 (YS-4). A possible reason is that the thermal degradation was more severe, and both the crystalline and amorphous regions of cellulose were destroyed, thus reducing the crystallite size during the thermal modification process. However, the thermal stability of the amorphous area of spruce after heat treatment was inferior, which caused the reduction of the amorphous area, thereby increasing the *CrI*. The *CrI* and crystallinity width of the heat-treated poplar and spruce were related to their L^* values, and the change rules were consistent. When the *CrI* of the thermally modified poplar and spruce reached the maximum, their color parameters were at the same level (YK-6: L^* = 37.55, a^* = 8.04, b^* = 13.06; YS-5: L^*= 34.15, a^* = 9.14, b^* = 10.81). The obtained *CrI* and crystallinity region width of heat-treated poplar and spruce in relationship with the L^* value is shown in Figure5a3 and b3. A Gaussian fit was used to fit the equation between the L^* values and the *CrI*, and crystallinity region width of the heat-treated wood. Therefore, it was further verified that there is a close relationship between L^* values and *CrI*, and crystallinity region width of the heat-treated wood, which provides a theoretical basis for predicting the mechanical properties of heat-treated wood based on its L^* values.

3.4. SEM structural analysis

Figure 6 shows surface micrographs of the transverse surfaces of untreated and heat-treated poplar. The transverse surface of the untreated poplar was smooth, the cells were arranged neatly, and the structure

was very complete. After thermal modification under different conditions, as the L^* value of the heat-treated poplar decreased, the surface of the cell wall gradually became rough, and the structure of the cell wall was squeezed, resulting in slight deformation. In addition, tiny cracks appeared between the middle lamella, some cells shrank and radially cracked, and the cell walls were partially destroyed. When the L^* of the heat-treated poplar dropped to the lowest value of 32.23 (YK-7), the degree of cell structure damage was greater. From the transverse surface of YK-7, it can be observed that the cells collapsed and deformed, the thickness of the cell wall became thinner, cracks were generated, and the cracks in the middle lamella increased **(Figure 6)**. The changes of cell wall thickness and morphology of wood after heat treatment have a great influence on its mechanical properties. By constructing a response relationship between L^* values and cell thickness of heat-treated wood, it provides a theoretical basis for predicting the mechanical properties of heat-treated wood based on the L^* values. However, lignin softening and massive degradation of hemicellulose destroys the linkages between hemicellulose and lignin and cellulose and reduces the number of hemicellulose and cellulose linkages. The increase in the number of breakpoints results in an increase in the degree of cleavage of the middle lamella in the heat-treated poplar (Van Zuylen et al. 1995). The radial thickness of the cell wall of the untreated poplar was 2.56 μm. Compared with the untreated wood, the radial thickness of the cell wall of the heat-treated poplar decreased gradually with decreasing L^* value. When the L^* value of heat-treated poplar decreased from 61.42 (YK-1) to 32.23 (YK-7), the radial thickness of its cell wall decreased from 2.29 μm to 1.65 μm **(Figure 8a1)**. With increasing heat treatment temperature and time, the degradation of the three main components and extractives in the cell wall of heat-treated wood intensified so the radial thickness of the cell wall decreased (Zauer et al. 2016; Stanzl-Tschegg et al. 2009).

Figure 7 shows surface micrographs of the transverse surfaces of untreated and heat-treated spruce. Spruce is coniferous wood, and the distinction between earlywood and latewood is very obvious. To elucidate the response relationships between the L^* of heat-treated wood and its cell structure morphology and radial thickness of the cell wall, the relationships between the L^* of wood under different treatments and the cell structure morphology and radial thickness of earlywood and latewood cell walls were analyzed. The cells of untreated earlywood and latewood spruce were neatly arranged, and the cell structure was complete. SEM analysis of the transverse surfaces of heat-treated spruce wood showed that microstructural changes clearly occurred. After thermal modification under different conditions, as the L^* value of the heat-treated spruce wood decreased, the surface of the cell walls of earlywood and latewood gradually became rough, a few burrs appeared, the cell structure began to deform slightly, and the middle lamella gradually exhibited tiny cracks. When the L^* of the heat-treated spruce dropped to the lowest value of 30.86 (YS-7), the degree of cell structure damage was greater. From the transverse surface of earlywood and latewood of YS-7, it can be observed that the cells collapsed and deformed, and the radial thickness of the cell wall became thinner. Among them, the deformation degree of earlywood cells was higher than that of latewood cells, and cracks appeared in the middle lamella layer **(Figure 7)**.

The radial thickness of the earlywood cell wall of untreated spruce was 2.21 μm. The radial thickness of the cell wall of spruce earlywood after heat treatment decreased with decreasing L^* value **(Figure 8b1)**. When the L^* of heat-treated spruce decreased from 58.59 (YS-1) to 34.15 (YS-5), the radial thickness of the earlywood cell wall did not decrease significantly, fluctuating in the range of 2.17-1.98 μm. When the L^* further decreased to 33.62 (YS-6) and 30.86 (YS-7), the radial thickness started to decrease sharply **(Figure 8b1)**. A possible reason for this is that lignin undergoes a glass transition, resulting in adhesive forces that anchor degraded cell wall components and volatile substances to the cell wall (Bakar et al. 2013; Ozcan et al. 2012). Therefore, the loss rate of the main components of the cell wall slowed to a certain extent, so the thickness of the cell wall did not significantly decrease. However, with the increase in thermally modification temperature and duration, the degradation of cellulose and hemicellulose intensified, and lignin no longer played a significant role in the hardening of cell walls, resulting in a significant decrease in the radial thickness of the cell wall of heat-treated spruce wood (Huang et al. 2012). Compared with the heat-treated spruce earlywood, the radial thickness of the cell wall of the latewood decreased sharply with the decrease in the L^* of the heat-treated wood. When the L^* of heat-treated spruce decreased from 58.59 (YS-1) to 30.86 (YS-7), the radial thickness of the latewood cell wall declined sharply from 5.31 μm to 2.70 μm.

From the above analysis, it can be seen that the L^* value of heat-treated poplar and spruce was closely related to the change in cell structure and cell wall radial thickness. A Gaussian fit was used to determine the equation between the L^* value and cell wall thickness variation for thermally modified poplar and spruce (**Figure 8a2 and b2**). A response relationship between the L^* value of thermally modified wood and their cell wall thickness was constructed. To further verify the response relationships between the L^* value and the cell structure and the radial thickness of the cell wall in the thermally treated wood, the correlation between the L^* value and the radial thickness of the cell wall was analyzed. From the analysis results in **Table 5**, it can be seen that there was an extremely significant positive correlation between the L^* value and the radial thickness of the cell wall of heat-treated poplar, and the correlation coefficient was 0.931. The correlation coefficient between the L^* value and the radial thickness of the latewood cell wall of heat-treated spruce was 0.948, which indicates an extremely significant correlation, but the correlation coefficient with the radial thickness of the earlywood cell wall was only 0.636, and the correlation was not significant. In summary, according to the response relationship between the L^* value of the heat-treated wood and the radial thickness of the cell wall, the degree of change of the cell structure and the radial thickness of the cell wall of heat-treated wood can be judged by the L^* value.

Table 5 Correlation analysis between L^* and the cell wall radial thickness of thermally treated wood.

Species	Index	Cell wall radial thickness
Poplar	L^*	0.931^{**}
Spruce (earlywood)	L^*	0.636
Spruce (latewood)	L^*	0.948^{**}

4. Conclusion

By analyzing the relationship between the color parameter L^* value and the main components and microstructure of the cell wall of heat-treated wood, the relationships between L^* and responses to thermal treatment were constructed. The relative cellulose content in heat-treated poplar was significantly negatively correlated with L^* value, while that of heat-treated spruce was not significantly correlated with L^* value. The L^* values of poplar and spruce after heat treatment both showed significant positive correlations with the relative hemicellulose and lignin contents, and it had the best response relationship with lignin. The *CrI* and crystalline size of poplar and spruce after thermal modification first increased and then reduced with the reduce of L^* value, and the L^* values had the best response relationship with their crystallite size. The shrinkage deformation and radial cracking of the cells of poplar and spruce after thermally modification became increasingly obvious as the L^* value of thermal modification gradually decreased. The L^* value of heat-treated poplar had an extremely significant positive correlation with its cell wall thickness, and this correlation was only found in latewood, which was further demonstrated by the Gaussian fitting formula. There was a close correlation between the change in the main components and the microstructure of the cell wall of the heat-treated wood and its mechanical strength. The constructed response relationships between the color parameters of heat-treated wood and its main components and the microstructure of the cell wall provide a theoretical basis for accurate predictions and nondestructive testing of the mechanical properties of thermally modified wood using color parameters as a rapid detection indicator.

Declarations

Declaration of Competing Interest

The authors declare that they have no known competing financial interests or personal relationships that could have appeared to influence the work reported in this paper.

Acknowledgments

This study was supported by the National Natural Science Foundation of China (31971590) Fundamental Research Funds for the Central Universities (2452019057) and Doctoral research start-up fee of Northwest A & F University (2452022123).

References

1. Ahajji A, Diouf P N, Aloui F et al. (2009) Influence of heat treatment on antioxidant properties and colour stability of beech and spruce wood and their extractives. Wood Sci. Technol. 43(1): 69-83. https://doi.org/10.1007/s00226-008-0208-3
2. Akgul M, Gumuskaya E, Korkut S (2007) Crystalline structure of heat-treated Scots pine [Pinus sylvestris L.] and Uludag fir [Abies nordmanniana (Stev.) subsp bornmuelleriana (Mattf.)] wood. Wood Science and Technology 41(3): 281-289. 10.1007/s00226-006-0110-9
3. Aydin I, Colakoglu G (2005) Effects of surface inactivation, high temperature drying and preservative treatment on surface roughness and colour of alder and beech wood. Applied Surface Science 252(2): 430-440. https://doi.org/10.1016/j.apsusc.2005.01.022
4. Bakar B, Hiziroglu S, Tahir P (2013) Properties of some thermally modified wood species. Materials & Design 43: 348-355. https://doi.org/10.1016/j.matdes.2012.06.054
5. Bekhta P, Niemz P (2003) Effect of high temperature on the change in color, dimensional stability and mechanical properties of spruce wood. Holzforschung 57(5): 539-546. https://doi.org/10.1515/HF.2003.080
6. Brischke C, Welzbacher CR, Brandt K, Rapp AO (2007) Quality control of thermally modified timber: interrelationship between heat treatment intensities and CIE L* a* b* color data on homogenized wood samples. Holzforschung 61(1): 19-22. https://doi.org/10.1515/HF.2007.004
7. Bhuiyan M, Rabbani T, Hirai N, Sobue N, (2000) Changes of crystallinity in wood cellulose by heat treatment under dried and moist conditions. Journal of Wood Science 46(6): 431-436. https://doi.org/10.1007/BF00765800
8. Bytner O, Drożdżek M, Laskowska A, Zawadzki J (2022) Temperature, Time, and Interactions between Them in Relation to Colour Parameters of Black Poplar (Populus nigra L.) Thermally Modified in Nitrogen Atmosphere. Materials 15(3): 824. https://doi.org/10.3390/ma15030824
9. Cademartori P, dos Santos P, Serrano L, Labidi J, Gatto D (2013) Effect of thermal treatment on physicochemical properties of Gympie messmate wood. Industrial Crops and Products 45: 360-366. https://doi.org/10.1016/j.indcrop.2012.12.048
10. Chen S, Wang J, Liu Y, Chen Z, Lei Y, Yan L (2022) The relationship between color and mechanical properties of heat-treated wood predicted based on support vector machines model. Holzforschung 76(11-22): 994-1002. 10.1515/hf-2022-0075
11. Colom X, Carrillo F, Nogués F, Garriga P (2003) Structural analysis of photodegraded wood by means of FTIR spectroscopy. Polym. Degrad. Stabil. 80: 543-549. https://doi.org/10.1016/S0141-3910(03)00051-X
12. Dennis J, Morén T (2006) The potential of colour measurement for strength prediction of thermally treated wood. Holz als Roh- und Werkstoff 64 (2): 104-110.
13. Esteves B, Marques A V, Domingos I, & Pereira H (2007) Influence of steam heating on the properties of pine (Pinus pinaster) and eucalypt (Eucalyptus globulus) wood. Wood Sci. Technol. 41(3): 193-

207. https://doi.org/10.1007/s00226-006-0099-0

14. Esteves B, Velez Marques A, Domingos I, Pereira H (2008) Heat-induced colour changes of pine (Pinus pinaster) and eucalypt (Eucalyptus globulus) wood. Wood Sci. Technol. 42(5): 369-384. https://doi.org/10.1007/s00226-007-0157-2
15. Esteves B, Pereira H (2009) Wood modification by heat treatment: A review. BioResources 4(1): 370-404.
16. Esteves B, Marques A, Domingos I, Pereira H (2013) Chemical changes of heat treated pine and eucalypt wood monitored by FTIR. Maderas Cienc. Tecnol. 15(2): 245-258.
17. Endo K, Obataya E, Zeniya N, Matsuo M (2016) Effects of heating humidity on the physical properties of hydrothermally treated spruce wood. Wood Sci. Technol. 50(6): 1161-1179.
18. Faix O (1991) Classification of lignins from different botanical origins by FTIR spectroscopy. Holzforschung 45: 21-27.
19. French A (2014) Idealized powder diffraction patterns for cellulose polymorphs. Cellulose 21(2): 885-896.
20. Ge S, Wu Y, Peng W et al. (2020) High pressure CO2 hydrothermal pretreatment of peanut shells for enzymatic hydrolysis conversion into glucose. Chem. Eng. J. 385: 123949. https://doi.org/10.1016/j.cej.2019.123949
21. González-Peña M M, Hale M D (2009a) Colour in thermally modified wood of beech, Norway spruce and Scots pine. Part 1: Colour evolution and colour changes. Holzforschung 63(4): 385-393. https://doi.org/10.1515/HF.2009.078
22. González-Peña M, Hale M (2009b) Colour in thermally modified wood of beech, Norway spruce and Scots pine. Part 2: property predictions from colour changes. Holzforschung 63(4): 394-401. https://doi.org/10.1515/HF.2009.077
23. Gunduz G, Aydemir D, Karakas G (2009) The effects of thermal treatment on the mechanical properties of wild Pear (Pyrus elaeagnifolia Pall.) wood and changes in physical properties. Mater. & Des. 30(10): 4391-4395. https://doi.org/10.1016/j.matdes.2009.04.005
24. Hakkou M, Pétrissans M, Gérardin P, Zoulalian A (2006) Investigations of the reasons for fungal durability of heat-treated beech wood. Polym. Degrad. Stab. 91: 393-397.
25. Hillis W E (1984) High temperature and chemical effects on wood stability. Wood Sci. Technol. 18(4): 281-293. https://doi.org/10.1007/BF00353364
26. Huang X, Kocaefe D, Kocaefe Y, Boluk Y, Pichette A (2012) Study of the degradation behavior of heat-treated jack pine (Pinus banksiana) under artificial sunlight irradiation. Polymer Degradation and Stability 97(7): 1197-1214. https://doi.org/10.1016/j.polymdegradstab.2012.03.022
27. Humar M, Repiˇc R, Kržišnik D et al. (2020) Quality Control of Thermally Modified Timber Using Dynamic Vapor Sorption (DVS) Analysis. Forests 11(6)L: 666. https://doi.org/10.3390/f11060666
28. Johansson D, Morén T (2006) The potential of colour measurement for strength prediction of thermally treated wood. Holz als Roh-und Werkstoff 64(2): 104-110. https://doi.org/10.1007/s00107-

005-0082-8

29. Kacik F, Luptáková J, Šmíra P et al. (2016) Chemical alterations of pine wood lignin during heat sterilization. BioResources 11(2): 3442-3452.
30. Kamdem D, Pizzi A, Jermannaud A (2002) Durability of heat-treated wood. Holz als Roh-und Werkstoff 60(1): 1-6.
31. Korkut S, Kök M S, Korkut D S, Gürleyen T (2008) The effects of heat treatment on technological properties in Red-bud maple (Acer trautvetteri Medw.) wood. Bioresource technology 99(6): 1538-1543. https://doi.org/10.1016/j.biortech.2007.04.021
32. Li J, Ma E (2021) Influence of heat treatment and delignification on hygroscopicity limit and cell wall saturation of southern pine wood. J For Eng. 6(3): 61-68.
33. Lin B, Colin B, Chen W et al. (2018) Thermal degradation and compositional changes of wood treated in a semi-industrial scale reactor in vacuum. Journal of Analytical and Applied Pyrolysis 130: 8-18.
34. Lu J, Jiang P, Chen Z, Li L (2020) Characteristic analysis of flame retardant particleboard using three methods of combustion performance evaluation. J. For. Eng. 5: 28-34.
35. Mitchell P H (2007) Irreversible property changes of small loblolly pine specimens heated in air nitrogen or oxygen Wood and Fiber Science 20(3): 320-335.
36. Moharram M, Mahmoud O (2008) FTIR Spectroscopic Study of the Effect of Microwave Heating on the Transformation of Cellulose I into Cellulose II during Mercerization. Journal of Applied Polymer Science 107(1): 30-36.
37. Nasir V, Nourian S, Avramidis S, Cool J (2019a) Stress wave evaluation for predicting the properties of thermally modified wood using neuro-fuzzy and neural network modeling. Holzforschung, 73(9): 827-838. https://doi.org/10.1515/hf-2018-0289
38. Nasir V, Nourian S, Avramidis S, Cool J (2019b) Classification of thermally treated wood using machine learning techniques. Wood Science and Technology 53(1): 275-288. https://doi.org/10.1007/s00226-018-1073-3
39. Nuopponen M, Vuorinen T, Jämsä S, Viitaniemi P (2005) Thermal modifications in softwood studied by FT-IR and UV resonance Raman spectroscopies. Journal of Wood Chemistry and Technology 24(1): 13-26. https://doi.org/10.1081/WCT-120035941
40. Obataya E, Tanaka F, Norimoto M, Tomita B (2000) Hygroscopicity of heat-treated wood, 1: Effects of after-treatments on the hygroscopicity of heat-treated wood. Journal of the Japan Wood Research Society (Japan) 46(2): 77-87.
41. Okon K E, Lin F, Lin X et al. (2018) Modification of Chinese fir (Cunninghamia lanceolata L.) wood by silicone oil heat treatment with micro-wave pretreatment. European Journal of Wood and Wood Products 76(1): 221-228. https://doi.org/10.1007/s00107-017-1165-z
42. Ozcan S, Ozcifci A, Hiziroglu S, Toker H (2012) Effects of heat treatment and surface roughness on bonding strength. Constr. Build. Mater. 33: 7-13. https://doi.org/10.1016/j.conbuildmat.2012.01.008

43. Özgenç Ö, Durmaz S, Boyaci I, Eksi-Kocak H (2017) Determination of chemical changes in heat-treated wood using ATR-FTIR and FT Raman spectrometry. Spectrochim. Acta A Mol. Biomol. Spectrosc. 171: 395-400.
44. Poletto M, Zattera A, Forte M, Santana R (2012) Thermal decomposition of wood: Influence of wood components and cellulose crystallite size. Bioresource Technology 109: 148-153. https://doi.org/10.1016/j.biortech.2011.11.122
45. Popescu M, Froidevaux J, Navi P, Popescu C (2013) Structural modifications of Tilia cordata wood during heat treatment investigated by FTIR and 2D IR correlation spectroscopy. J. Mol. Struct. 1033: 176-186.
46. Salca E, Hiziroglu S (2014) Evaluation of hardness and surface quality of different wood species as function of heat treatment. Mater. & Des. 62: 416-423. https://doi.org/10.1016/j.matdes.2014.05.029
47. Salca E A, Kobori H, Inagaki T et al. (2016) Effect of heat treatment on colour changes of black alder and beech veneers. J Wood Sci. 62(4): 297-304. https://doi.org/10.1007/s10086-016-1558-3
48. Sandberg D, Haller P, Navi P (2013) Thermo-hydro and thermo-hydro-mechanical wood processing: An opportunity for future environmentally friendly wood products. Wood Material Science & Engineering 8(1): 64-88. https://doi.org/10.1080/17480272.2012.751935
49. Schemer P (1918) Bestimmung der Grosse und der Inneren Struktur von Kolloidteilchen Mittels Rontgenstrahlen, Nachrichten von der Gesellschaft der Wissenschaften, Gottingen, Math. Phys. 2: 98-100.
50. Schnabel T, Zimmer B, Petutschnigg A J, Schonberger S (2007) An approach to classify thermally modified hardwoods by color. Forest Prod. 57(9): 105.
51. Schwarze R, Spycher M (2005) Resistance of thermo-hygro-mechanically densified wood to colonisation and degradation by brown-rot fungi. Holzforschung 59(3): 358-363. https://doi.org/10.1515/HF.2005.059
52. Segal L, Creely J, Martin Jr A, Conrad C (1959) An empirical method for estimating the degree of crystallinity of native cellulose using the X-ray diffractometer. Textile research journal 29(10): 786-794. https://doi.org/10.1177/004051755902901003
53. Sikora A, Kačík F, Gaff M et al (2018) Impact of thermal modification on color and chemical changes of spruce and oak wood. J Wood Sci. 64(4): 406-416. https://doi.org/10.1007/s10086-018-1721-0
54. Spiridon I, Teaca C, Bodirlau R (2011) Structural changes evidenced by FTIR spectroscopy in cellulosic materials after pretreatment with ionic liquid and enzymatic hydrolysis. BioResources 6: 400-413.
55. Srinivas K, Pandey K (2012) Photodegradation of thermally modified wood. J Photoch. Photobio. B. 117: 140-145. https://doi.org/10.1016/j.jphotobiol.2012.09.013
56. Stanzl-Tschegg S, Beikircher W, Loidl D (2009) Comparison of mechanical properties of thermally modified wood at growth ring and cell wall level by means of instrumented indentation tests. Holzforschung 63(4): 443-448.

57. Sundqvist B, Morén T (2002) The influence of wood polymers and extractives on wood colour induced by hydrothermal treatment. European Journal of Wood and Wood Products 60(5): 375-376.
58. Sundqvist B, Karlsson O, Westermark U (2006) Determination of formic-acid and acetic acid concentrations formed during hydrothermal treatment of birch wood and its relation to colour, strength and hardness. Wood Sci. Technol. 40(7): 549-561. https://doi.org/10.1007/s00226-006-0071-z
59. Tjeerdsma B, Militz H 2005. Chemical changes in hydrothermal treated wood: FTIR analysis of combined hydrothermal and dry heat-treated wood. Holz als roh-und Werkstoff, 63(2), 102-111. https://doi.org/10.1007/s00107-004-0532-8
60. Torniainen P, Jones D, Sandberg D (2021) Colour as a quality indicator for industrially manufactured ThermoWood®. Wood Mater, Sci, Eng. 16(4): 287-289. https://doi.org/10.1080/17480272.2021.1958920
61. Toba K, Yamamoto H, Yoshida M (2013) Crystallization of cellulose microfibrils in wood cell wall by repeated dry-and-wet treatment, using X-ray diffraction technique. Cellulose 20(2): 633-643.
62. Vartanian E, Barres O, Roque C (2015) FTIR spectroscopy of woods: a new approach to study the weathering of the carving face of a sculpture. Spectrochim. Acta A Mol. Biomol. Spectrosc. 136: 1255-1259.
63. Van Zuylen A (1995) Platonische Liefde voor hout. Chemisch Maga-zine, 212-213.
64. Wang X, Huang Y, Lv C et al. (2022) Multi-scale investigation of the mechanical properties of Loblolly pine wood at elevated temperature. Wood Mater Sci Eng. 18 (2): 517-524. https://doi.org/10.1080/17480272.2022.2053203
65. Wei L, McDonald A G, Stark N M (2015) Grafting of bacterial polyhydroxybutyrate (PHB) onto cellulose via in situ reactive extrusion with dicumyl peroxide. Biomacromolecules 16(3): 1040-1049. https://doi.org/10.1021/acs.biomac.5b00049
66. Welzbacher C, Brischke C, Rapp A (2007) Influence of treatment temperature and duration on selected biological, mechanical, physical and optical properties of thermally modified timber. Wood Material Science & Engineering 2(2): 66-76.
67. Westermark U, Samuelsson B, Lundquist K (1995) Homolytic cleavage of the β-ether bond in phenolic β-O-4 structures in wood lignin and in guaiacylglycerol-β-guaiacyl ether. Research on chemical intermediates 21(3): 343-352. https://doi.org/10.1007/BF03052263
68. Wikberg H, Maunu S L (2004) Characterisation of thermally modified hard-and softwoods by 13C CPMAS NMR. Carbohydrate polymers 58(4): 461-466. https://doi.org/10.1016/j.carbpol.2004.08.008
69. Willems W, Lykidis C, Altgen M, Clauder L (2015) Quality control methods for thermally modified wood. Holzforschung 69(7): 875-884. https://doi.org/10.1515/HF-2014-0185
70. Windeisen E, Wegener G (2008) Behaviour of lignin during thermal treatments of wood. Industrial crops and products 27(2): 157-162. https://doi.org/10.1016/j.indcrop.2007.07.015
71. Xu J, Zhang Y, Shen Y et al. (2019) New perspective on wood thermal modification: Relevance between the evolution of chemical structure and physical-mechanical properties, and online analysis

of release of VOCs. Polymers 11(7): 1145.

72. Yan L, Morrell J J (2019) Kinetic color analysis for assessing the effects of borate and glycerol on thermal modification of wood. Wood Sci. Technol. 53(1): 263-274. https://doi.org/10.1007/s00226-018-1072-4
73. Yang H, Yan R, Chen H, Lee D H, Zheng C (2007) Characteristics of hemicellulose, cellulose and lignin pyrolysis. Fuel 86(12-13): 1781-1788. https://doi.org/10.1016/j.fuel.2006.12.013
74. Yildiz S, Gezer E D, Yildiz U C (2006) Mechanical and chemical behavior of spruce wood modified by heat. Building and environment 41(12): 1762-1766. https://doi.org/10.1016/j.buildenv.2005.07.017
75. Zauer M, Meissner F, Plagge R, Wagenfuhr A (2016) Capillary pore-size distribution and equilibrium moisture content of wood determined by means of pressure plate technique. Holzforschung 70(2): 137-143.
76. Zheng A, Jiang L, Zhao Z et al. (2015) Impact of torrefaction on the chemical structure and catalytic fast pyrolysis behavior of hemicellulose lignin, and cellulose. Energy Fuel 29: 8027-8034.
77. Zheng Z, Zhao Z, Chang S et al. (2013) Effect of torrefaction on structure and fast pyrolysis behavior of corncobs. Bioresour. Technol. 128: 370-377.

Figures

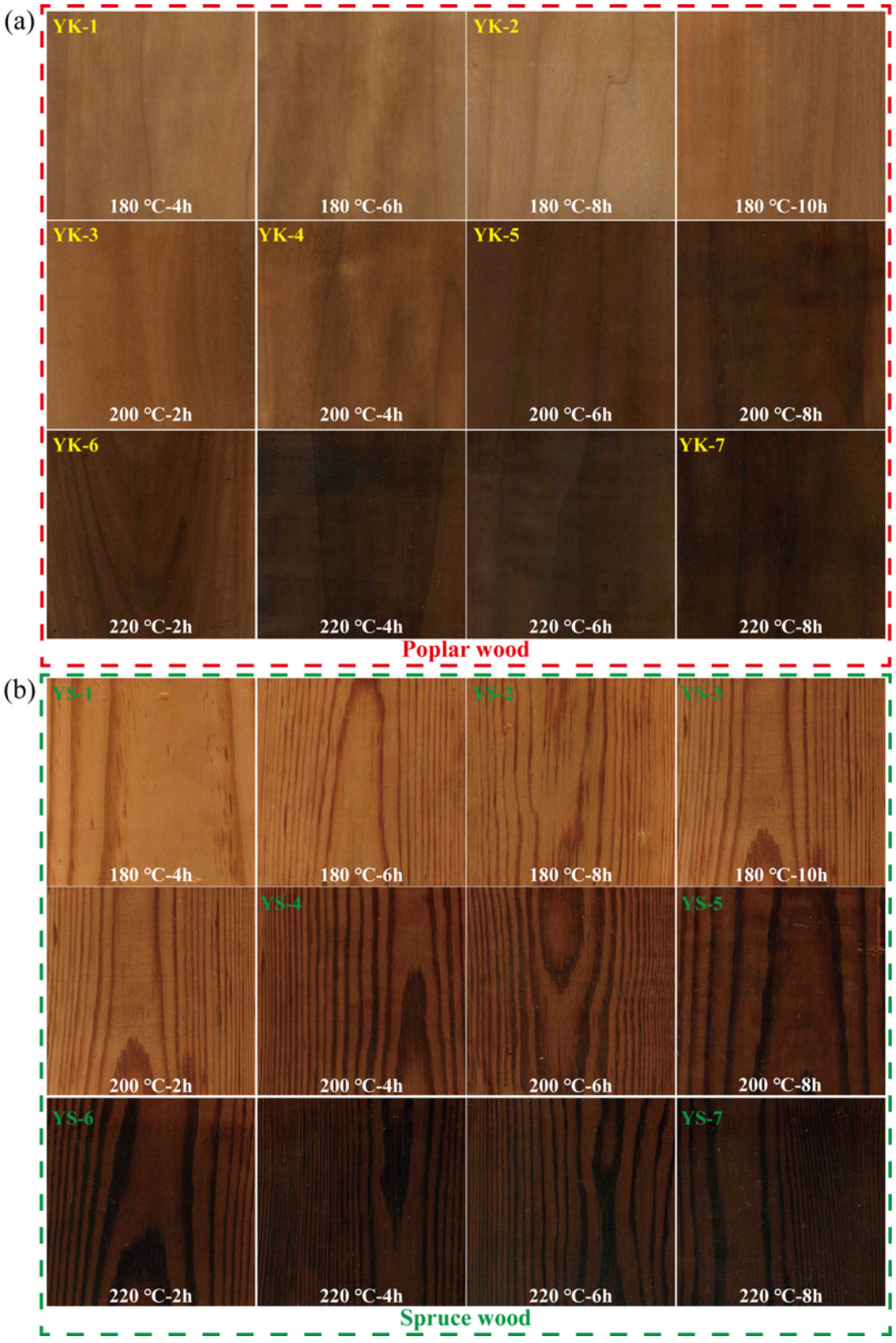

Figure 1

Surface color of thermally modified poplar (a) and spruce (b).

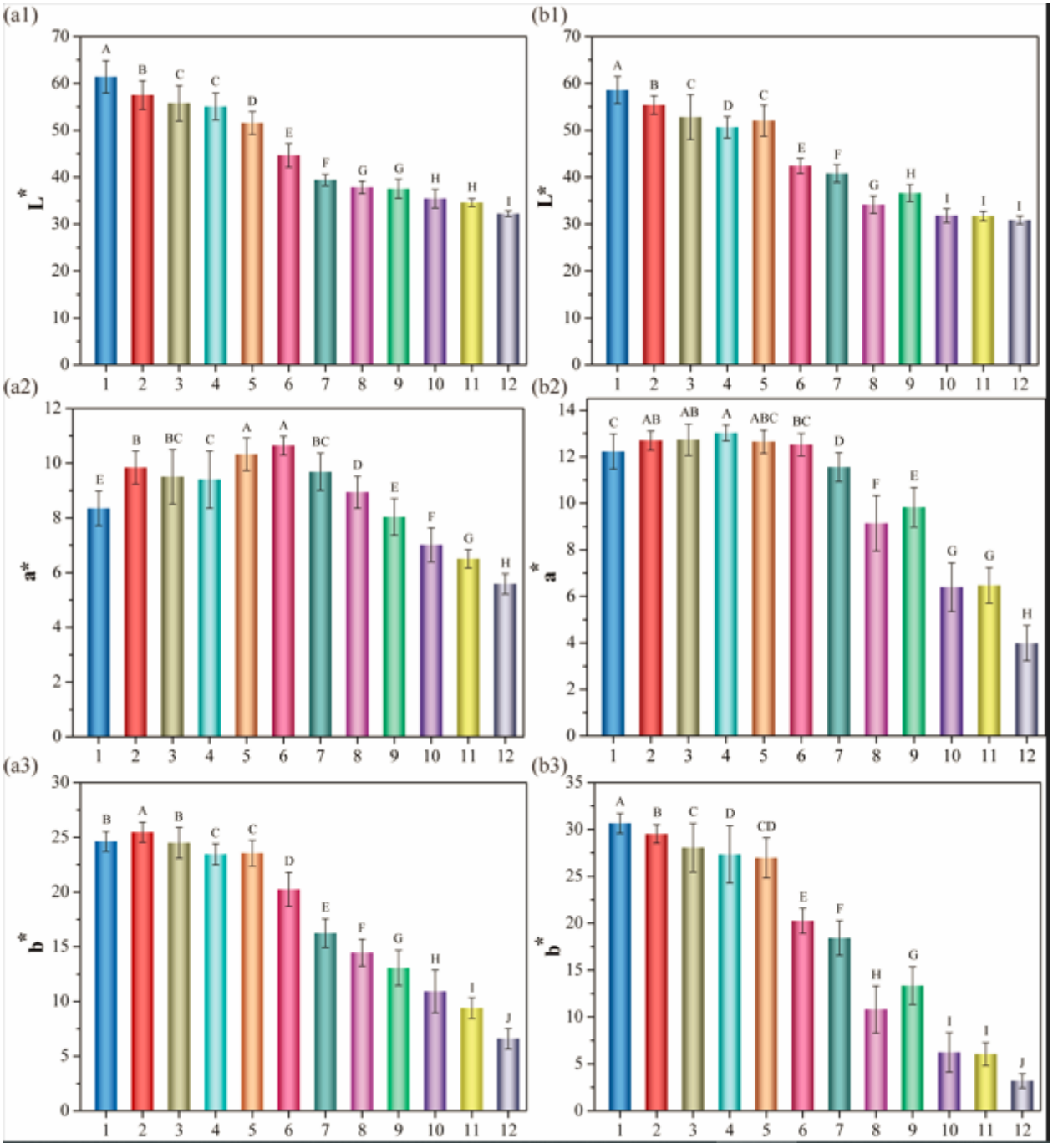

Figure 2

L^* values of thermally modified poplar and spruce.

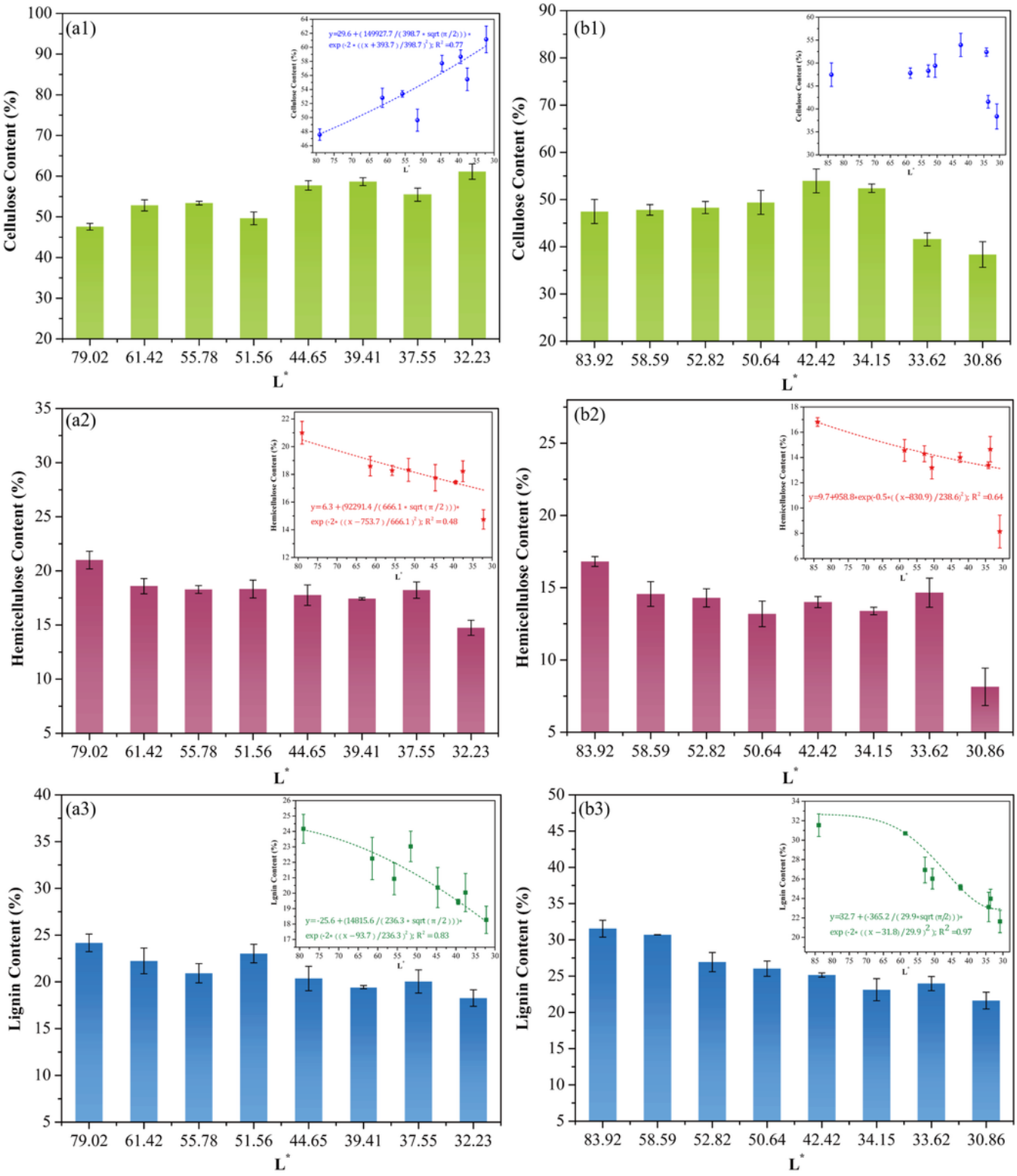

Figure 3

Chemical composition of the poplar (a1, a2, a3) and spruce (b1, b2, b3)

after thermal treatment.

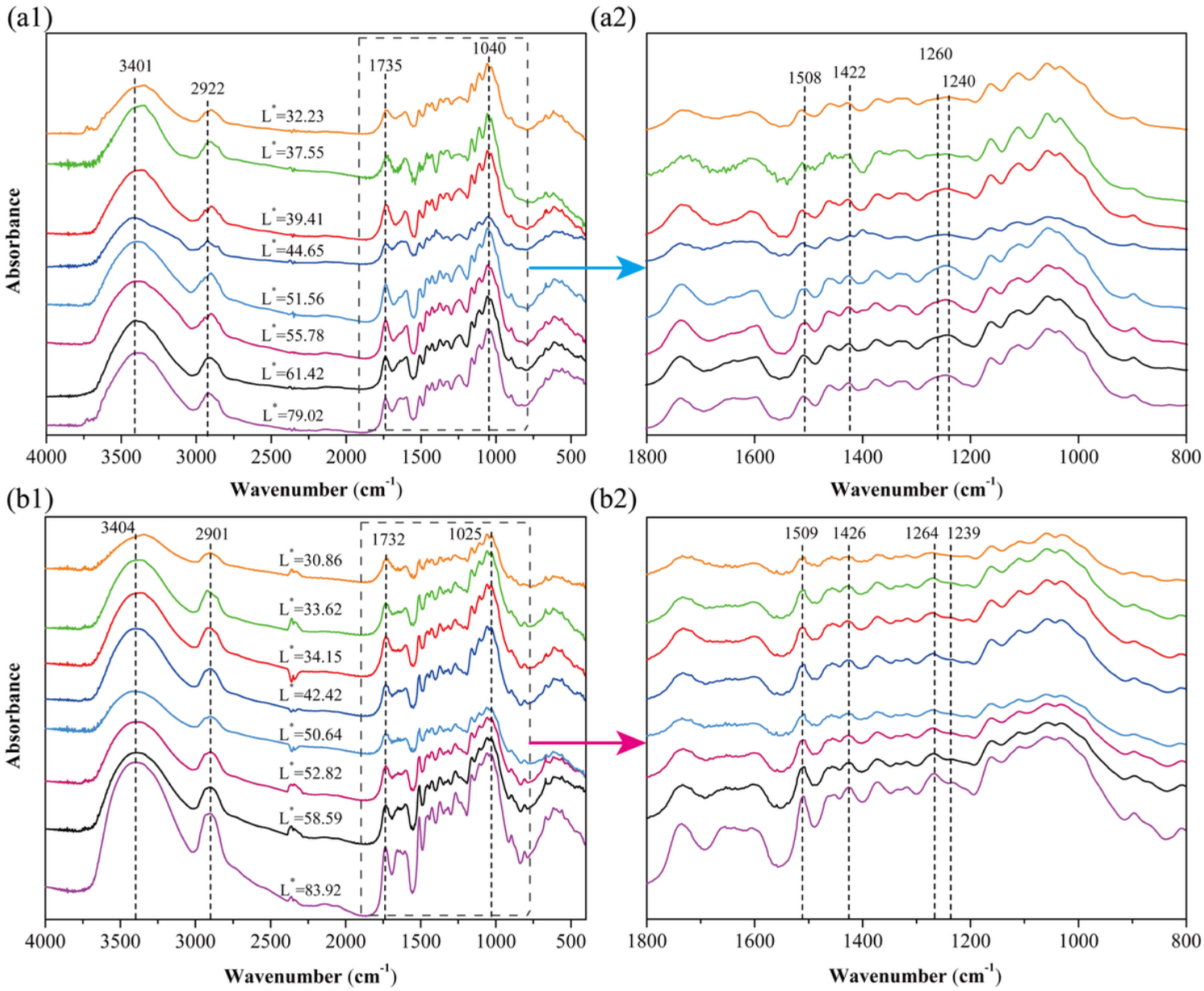

Figure 4

FTIR spectra of poplar and spruce wood after thermal treatment.

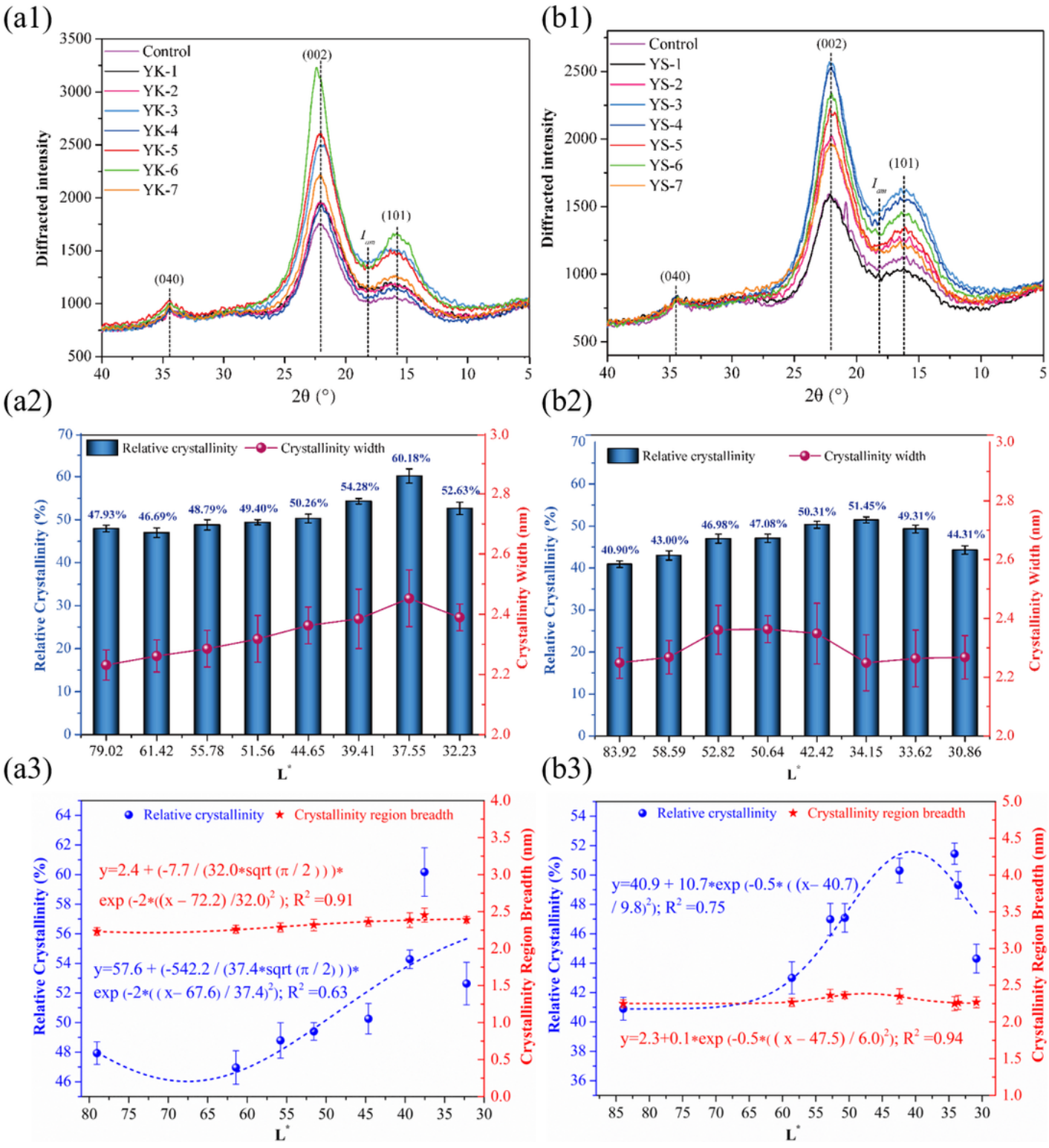

Figure 5

XRD spectra (a1: poplar, b1: spruce), *CrI* and crystallinity region width (a2: poplar, b2: spruce), and the obtained *CrI* and crystallinity region width in relationship with the L^* value (a3: poplar, b3: spruce) of the samples.

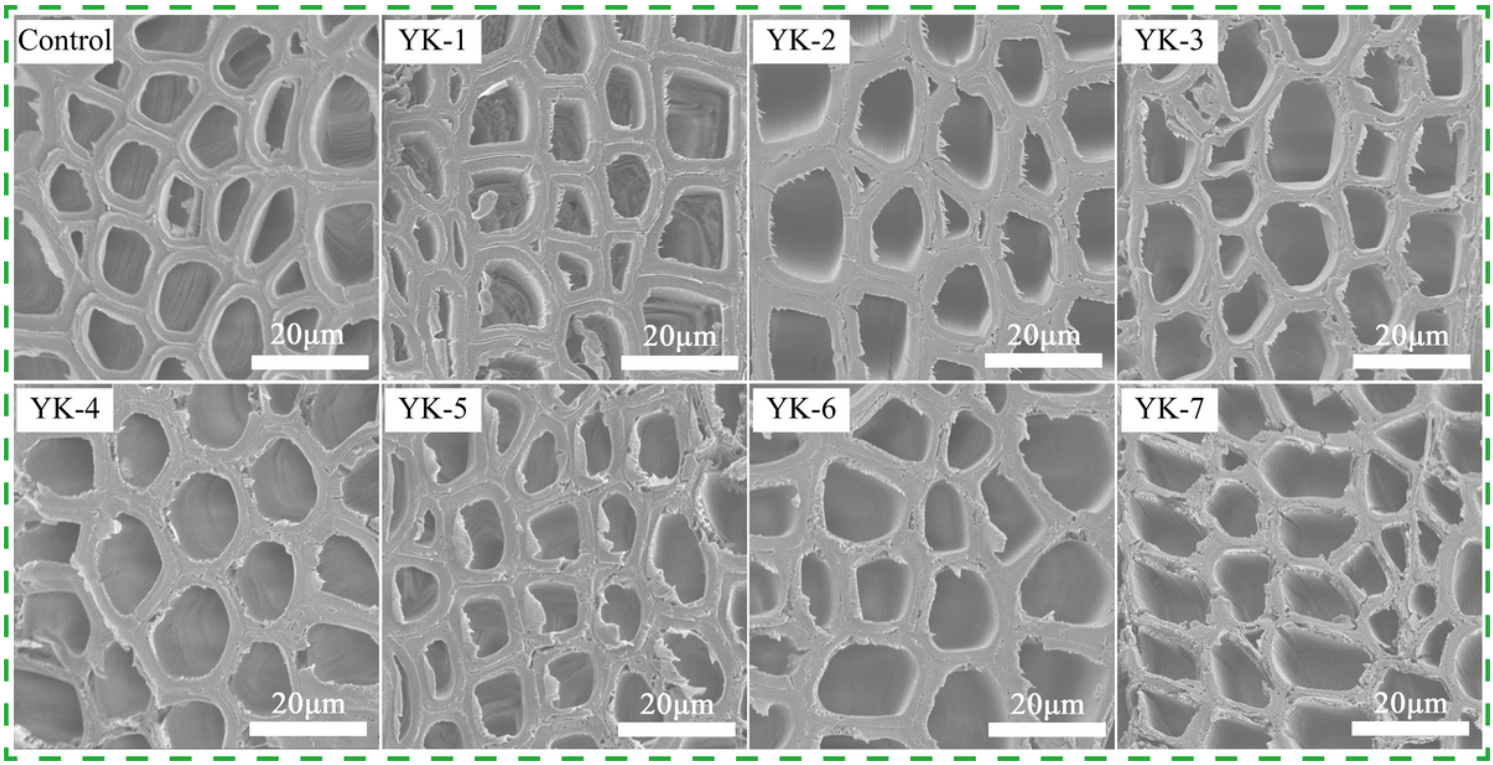

Figure 6

SEM images of untreated and heat-treated poplar wood.

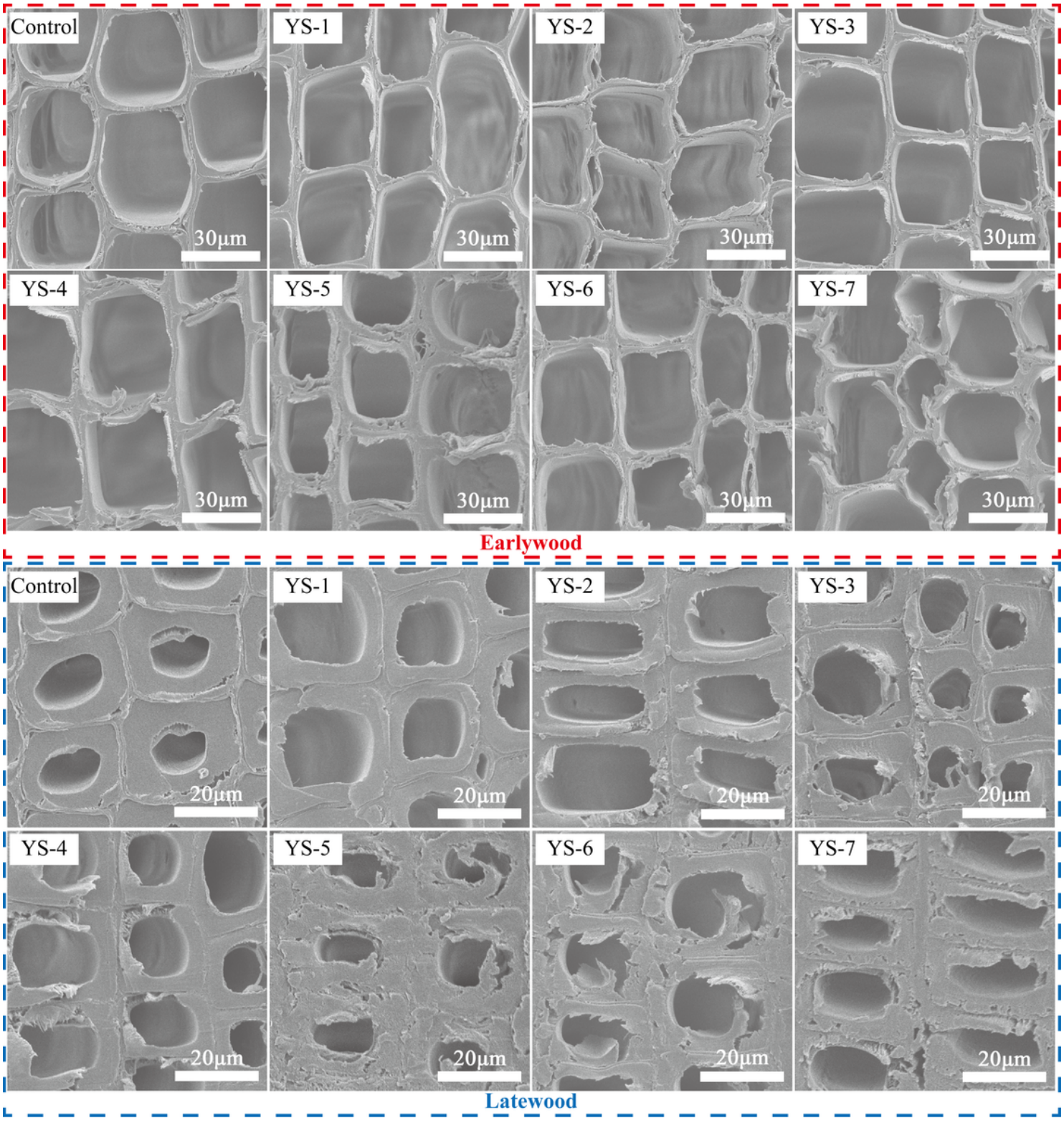

Figure 7

SEM images of untreated and heat-treated earlywood and latewood spruce.

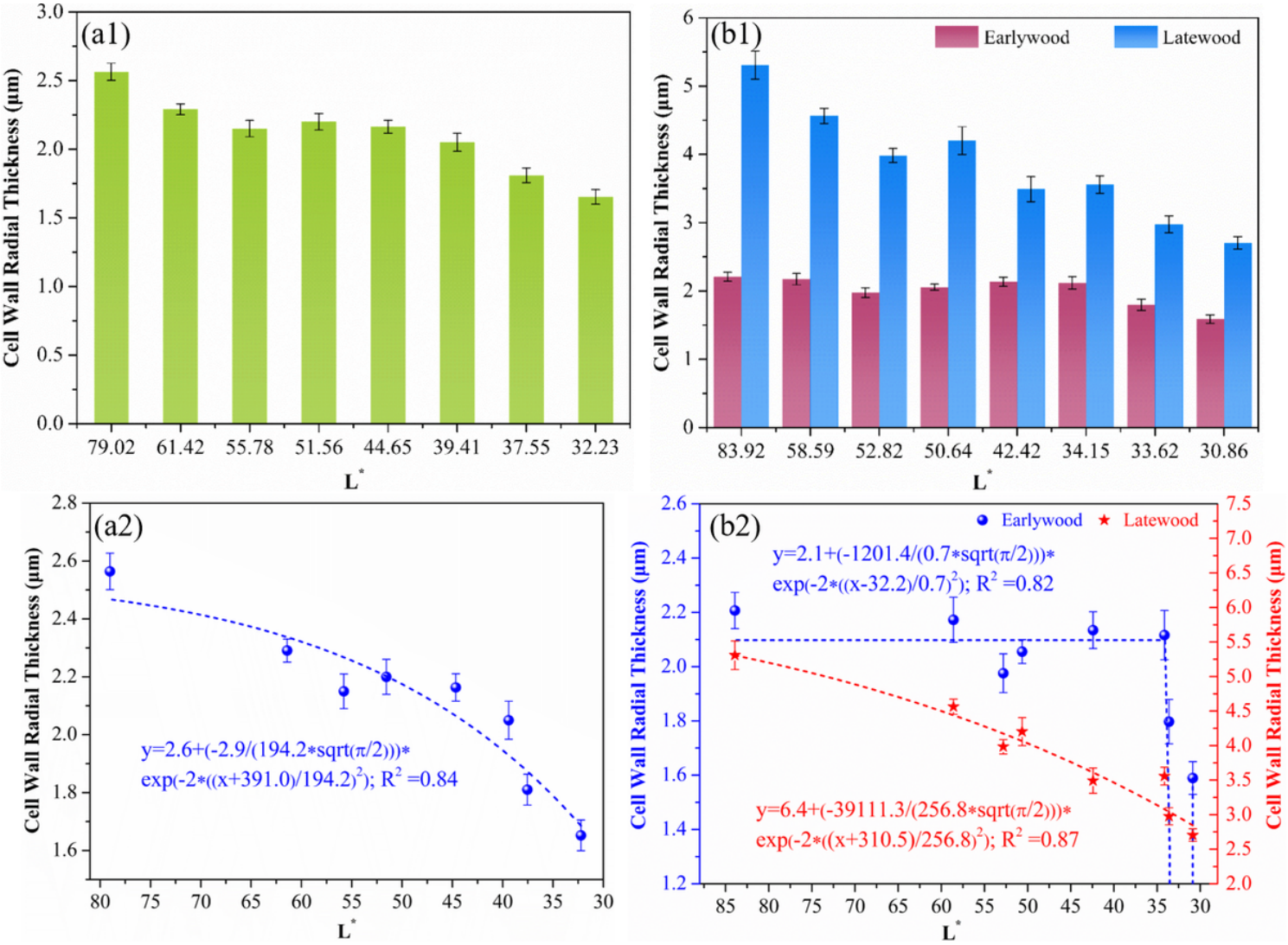

Figure 8

Cell wall radial thickness of poplar (a1), early wood and late wood spruce (b1), and the obtained cell wall radial thickness in relationship with the L* value (a2: poplar, b2: spruce) of the heat-treated wood.